Molecular Therapy
Oncolytics
Original Article

AMERICAN SOCIETY of GENE & CELL THERAPY

In Situ Therapeutic Cancer Vaccination with an Oncolytic Virus Expressing Membrane-Tethered IL-2

Weilin Liu,[1,2,3,4] Enyong Dai,[3,4,5] Zuqiang Liu,[3,4] Congrong Ma,[3,4] Zong Sheng Guo,[3,4] and David L. Bartlett[3,4]

[1]The Third Xiangya Hospital, Central South University, Changsha, Hunan, China; [2]Xiangya School of Medicine, Central South University, Changsha, Hunan, China; [3]Department of Surgery, University of Pittsburgh School of Medicine, Pittsburgh, PA, USA; [4]UPMC Hillman Cancer Center, Pittsburgh, PA, USA; [5]Department of Oncology and Hematology, China-Japan Union Hospital of Jilin University, Changchun, Jilin, China

Successful *in situ* therapeutic vaccination would allow locally delivered oncolytic virus (OV) to exert systemic immunologic effects on metastases and improve survival. We have utilized bilateral flank tumor models to determine the most efficacious regimens of *in situ* vaccination. Intratumoral injection with membrane-tethered interleukin -2-armed OV (vvDD-mIL2) plus a Toll-like receptor 9 ligand (CpG) yielded systemic immunization and decreased tumor growth in a contralateral, noninjected tumor. Our main aims were to study the tumor immune microenvironment (TME) after vaccination and identify additional immune adjuvants that may improve the systemic tumor-specific immunity. Immunological profiles in the spleen showed an increased $CD8^+$ T cell/regulatory T cell (Treg) ratio and increased $CD11c^+$ cells after dual injection in one flank tumor. Concurrently, there was increased infiltration of tumor necrosis factor alpha (TNF-α)$^+CD8^+$ T cells and interferon gamma (IFN-γ)$^+CD4^+$ T cells and reduced CTLA-4^+PD-1^+CD8^+ T cells in the contralateral, noninjected tumor. The anti-tumoral activity depended on $CD8^+$ T cells and IFN-γ, but not $CD4^+$ T cells. Based on the negative immune components still existing in the untreated tumors, we investigated additional adjuvants: clodronate liposome-mediated depletion of macrophages plus anti-PD-1 therapy. This regimen dramatically reduced the tumor burden in the noninjected tumor and increased median survival by 87%, suggesting that inhibition/elimination of suppressive components in the tumor microenvironment (TME) can improve therapeutic outcomes. This study emphasizes the importance of immune profiling to design rational, combined immunotherapy regimens ultimately to impact patient survival.

INTRODUCTION

Oncolytic virus (OV)-mediated cancer therapy has shown promise. Imlygic, a herpes simplex virus expressing the granulocyte-macrophage colony-stimulating factor, has been the only drug of its class approved by the US Food and Drug Administration (FDA). It was approved as a local intratumoral (i.t.) injection to treat patients with advanced melanoma.[1] This local injection, however, resulted in an improvement in overall survival, suggesting that *in situ* cancer vaccination may have resulted in a systemic immune response that impacted micro-metastatic disease.[2–4] OVs can induce an immunogenic cell death[5–7] and when combined with T cell-activating cytokine expression, can change the cancer-immune set point within the tumor, transforming a nonimmunogenic microenvironment into an immunogenic one.[8–10] The optimization of this effect with additional immune adjuvants may lead to a successful *in situ* vaccination strategy for low- or nonimmunogenic tumors.

We[11] and others[12] have shown that oncolytic vaccinia viruses (VVs) are highly promising OVs for cancer therapy. The vv double deletion (vvDD) is an OV with deleted viral genes encoding thymidine kinase (TK) and vaccinia growth factor. Its cancer selectivity was mediated through multiple mechanisms, as its replication was activated by epidermal growth factor receptor/Ras pathway signaling, cellular TK levels, and resistance to type I interferons (IFNs) in cancer cells.[13,14] Clinically, this virus vvDD has been shown to be safe, yet with limited therapeutic efficacy in patients with advanced solid cancers.[15,16] Many recent studies of OVs have emphasized the importance of enhancing tumor-specific immunity for improved results, including the use of immunogenic transgenes and combination with immune adjuvants.[17–19] In fact, several studies have shown that OVs themselves or in combination with immune-checkpoint blockade elicit systemic anti-tumor immunity.[20–28] The systemic anti-tumoral immunity thus generated, however, is usually not able to eradicate distant tumors. Therefore, other various combination strategies need to be explored to improve results. Recently, we designed a VV expressing membrane-bound interleukin -2 (vvDD-mIL2) by combining a glycosylphosphatidylinositol anchor with a rigid peptide linker. This virus leads to functional IL-2 expression on the tumor cell surface within the tumor tissue. It displayed high therapeutic efficacy in a variety of murine

Received 5 February 2020; accepted 15 April 2020;
https://doi.org/10.1016/j.omto.2020.04.006.

Correspondence: David L. Bartlett, MD, Department of Surgery, University of Pittsburgh School of Medicine, and UPMC Hillman Cancer Center, Pittsburgh, PA, USA.
E-mail: bartdl@upmc.edu
Correspondence: Zong Sheng Guo, PhD, Department of Surgery, University of Pittsburgh School of Medicine, and UPMC Hillman Cancer Center, Pittsburgh, PA, USA.
E-mail: guozs@upmc.edu

tumor models with no detectable toxic side effects.[9] It is possible that the combination of this potent and safe immunogenic virus with other immune adjuvants may lead to optimal systemic anti-tumor immunity and therapeutic efficacy.

In previous work, combined local injection of a Toll-like receptor 9 (TLR9) agonist and an agonistic anti-OX40 T cell-activating antibody led to the cure of multiple types of metastatic cancers in murine models.[29] Synthetic phosphorothionate oligodeoxynucleotides (ODNs) containing unmethylated CpG dinucleotides (CpG ODNs) are TLR9 agonists and have been developed for cancer therapy.[30,31] They function to activate both innate and adaptive immunity, and i.t. delivery induces a broad antigen-specific T cell response against the tumor.[32] Indeed, *in situ* vaccination with a TLR9 agonist induces systemic clinical responses in lymphoma patients.[33] Previous work has demonstrated that TLR3/9 ligands (polyinosinic:polycytidylic acid [poly I:C]/CpG) injected into a tumor during the effector phase of immunization effectively rescued the function of activated cluster of differentiation $CD8^+$ tumor-infiltrating lymphocytes and decreased the ratio and absolute number of regulatory T cells (Tregs) within the tumor, thus improving the anti-tumoral efficacy elicited by cancer vaccines.[34] Importantly, TLR9 signaling and T cell receptor (TCR) stimulation co-regulate $CD8^+$ T cell-associated programmed cell death protein 1 (PD-1) expression. Thus, TLR9 agonists may enhance the functionality of $CD8^+$ T cells.[35,36] In numerous studies, a TLR agonist by itself has shown limited efficacy, yet in combinations with other immune adjuvants, it provides a synergistic stimulus to elicit anti-tumor immunity.[29] This synergistic effect may be extended to the immune activity of OVs.

In the current study, we hypothesized that *in situ* therapeutic vaccination, using the combination of local delivery of vvDD-mIL2 and immune adjuvants, might lead to potent systemic anti-tumoral immunity and therapeutic efficacy in both treated and untreated tumor nodules. To achieve this goal, we utilized two murine models with bilateral syngeneic flank tumors, injected with the same number of tumor cells at the same time in both flanks. This represents a stringent model when compared to other studies, but it allows the study of the abscopal effect mediated by systemic anti-tumor immunity on the nontreated large tumor nodule from a distance. We then injected the immune therapy into one of the tumors and assessed the response in both the injected and noninjected ones, following the mice for overall survival after treatment. As oncolytic VV spreads from cell to cell without being released from the cell membrane, the contralateral tumor is free from viral infection, and any response is immunologically mediated. We explored the phenotype of immune cells infiltrating the noninjected tumor to understand better the mediators of the immune response and identify any suppressive factors that need to be addressed using additional systemic immune adjuvants.

RESULTS

The OV Elicits Anti-tumoral Immune Activity in Both Injected and Noninjected Tumor Nodules

We established separate nodules of subcutaneous (s.c.) MC38 colon cancer on both flanks of each mouse and then treated one of the two tumor nodules with an i.t. injection of VV expressing no transgene (vvDD) or membrane-bound IL-2 (vvDD-mIL2) (Figure S1). To confirm that the replicating virus did not spread to infect the untreated tumor, we examined expression of A34R as a viral marker gene using quantitative reverse transcription-polymerase chain reaction (qRT-PCR) on days 8 and 11 after viral injection. Results confirmed high levels of A34R mRNA expression in the injected nodules, but no expression was detected in the untreated nodules after treatment with either vvDD or vvDD-mIL2 (Figure 1A; Figure S2). Of note, both vvDD and vvDD-mIL2 induced regression of the MC38-luc tumor in the treated nodules ($p < 0.0001$ compared to phosphate-buffered saline [PBS]), whereas only vvDD-mIL2 significantly slowed the growth of the untreated nodule ($p < 0.001$) (Figure 1B).

Intratumoral OV Leads to Potent Systemic Anti-tumor Immunity

We examined the immunologic effects of vvDD and vvDD-mIL2 in the injected tumor, untreated tumor, and spleen. vvDD-mIL2 induced a higher percentage of $CD8^+$ T cells and higher numbers of activated $CD8^+$ T cells and PD-1^+CD8^+ T cells in both the treated and untreated nodules (Figures 1C–1E). Additionally, a time-course analysis of IFN-γ^+CD8^+ T cells in the untreated tumor demonstrated that vvDD-mIL2 treatment led to an increase relative to the PBS control on days 5 and 8 after viral injection, with a peak at day 8 (Figure 1F). These findings demonstrate that vvDD-mIL2 causes an activated T cell response in the untreated tumor, leading to a reduction in tumor growth. To identify the systemic tumor-specific immunity induced by the i.t. injection of OV, we isolated splenocytes from tumor-bearing mice receiving PBS, vvDD, or vvDD-mIL2 and restimulated with irradiated MC38-luc or control B16 cancer cells *in vitro* for 24 h, and an IFN-γ ELISpot (enzyme-linked immune absorbent spot) assay was performed. The results indicated that significantly increased numbers of activated and tumor-specific splenocytes were observed after vvDD-mIL2 treatment compared to PBS or vvDD treatment (Figures 2A and 2B). We separated the animals with high reactivity, intermediate reactivity, and low reactivity, depending on ELISpot assays (Figure 2B), and analyzed $CD8^+$ T cell infiltration and tumor response in the untreated tumors. Those with high ELISpot reactivity had increased CD8 infiltration (mRNA for CD8) and improved anti-tumor response compared to those with intermediate or low reactivity (Figures 2C and 2D).

In summary, these results suggest that vvDD-mIL2 elicited systemic anti-tumor immunity, leading to infiltration of activated T cells into the untreated tumor and resulting in a therapeutic effect. As vvDD-mIL2 displays more potent systemic immune reactivity than vvDD, we only studied vvDD-mIL2 in subsequent experiments.

Intratumoral Injection of vvDD-mIL2 Plus TLR9 Ligand Markedly Improves *In Situ* Therapeutic Vaccination in MC38 Colon and Lewis Lung Carcinoma Models

Numerous studies have shown that CpG (a TLR9 agonist), OX40 agonists, and anti-PD-1/PD-1 ligand (PD-L1) antibodies can function as an adjuvant to improve the activity of vaccines through different mechanisms.[37–39] Therefore, we examined different combinations

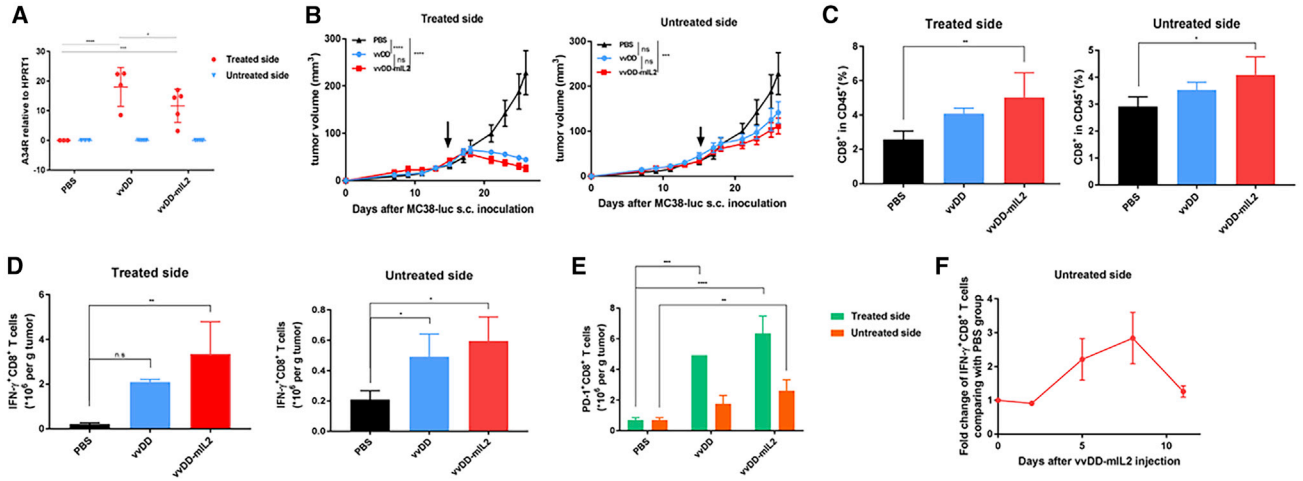

Figure 1. vvDD-mIL2 Generates Anti-tumoral Immune Activity and Augments i.t. Infiltration of CD8$^+$ T Cells in Both Local and Distant Tumors

(A) A qRT-PCR assay was performed to test the level of A34R mRNA on day 8 after i.t. injection of virus. (B) The growth curves of the s.c. MC38-luc tumor on both the treated and untreated side are shown. The virus was injected i.t. on day 16 (arrows) using 1.0e8 PFU/50 μL per mouse. (C–E) B6 tumor-bearing mice were sacrificed on day 8 post-virus treatment, and tumor tissues on both flanks were collected and analyzed for infiltrating CD8$^+$ T cells using flow cytometry. The percentage of CD8$^+$ cells in CD45$^+$ leukocytes from both sides is displayed (C), the quantities of IFN-γ$^+$CD8$^+$ (D), and PD-1$^+$CD8$^+$ T cells (E) per gram of tumor are shown. The fold changes of IFN-γ$^+$CD8$^+$ T cells from the untreated side compared to the PBS-treated group over time is shown (F). Values represent mean ± SD. Two-way ANOVA was used to analyze the statistical significance in (A) and (E) (*$p < 0.05$; **$p < 0.01$; ***$p < 0.001$; ****$p < 0.0001$; and ns, not significant). In other panels, we used one-way ANOVA (the standard symbols for p values are the same). This experiment has been repeated at least twice.

of local injections of vvDD-mIL2 with CpG, OX40 agonist antibody, and anti-PD-1 in our bilateral flank tumor model (Figure S3). After local injection of CpG and vvDD-mIL2, the injected tumor was completely eradicated in most of the mice, and no additional therapeutic effect was demonstrated with the addition of i.t. injection of OX86 (OX40 agonist antibody) (Figures S3A–S3D). Similarly, the best response in the untreated tumors was obtained from the combination treatment of CpG and vvDD-mIL2 without extra benefit from the addition of i.t. injection of anti-PD-1 (Figures S3E–S3H). These results also correlated with survival, where CpG plus vvDD-mIL2 treatment increased median survival by 27% −33% compared to PBS treatment (Figures S3D and S3H).

We repeated the experiment using vvDD-mIL2 and CpG i.t. injections, according to the schedules shown (Figure S4A), to confirm the previous findings and to examine the weight of the tumor nodules. With the consideration of both the treated and untreated sides, the combination of vvDD-mIL2 and CpG treatment worked better than monotherapy or PBS control (Figure 3A). Then, we examined an additional cohort for survival and found that vvDD-mIL2 plus CpG extended median survival by 32% compared to PBS treatment (Figure 3B). Another cohort of treated mice was sacrificed 1 day after the second injection of CpG, and tumor weight again verified the same conclusion (Figure 3C). To confirm this *in situ* therapeutic vaccination activity in another histology, we established bilateral s.c. Lewis lung carcinomas in B6 mice and treated them with the same regimens using the same dose and time schedule. We observed similar patterns of anti-tumoral response and prolongation of survival (Figures S4B and S4C).

In summary, these results demonstrate additive effects on the anti-tumor response in the untreated tumor when vvDD-mIL2 is combined with CpG injection into the contralateral tumor.

Immunologic Analysis of Combined vvDD-mIL2 Treatment and CpG Treatment

Next, we examined the impact of vvDD-mIL2 and CpG on splenocytes and the tumor microenvironment (TME) to understand the immunologic mechanisms induced by this combination (Table S1). 1 day after receiving all of the injections, the combination therapy led to a statistically significant increased ratio of cytotoxic T cells to Tregs in splenocytes and an increased percentage of CD11c$^+$ cells (dendritic cells [DCs] and other myeloid cells) (Figures 4A and 4B; Figure S5). However, the combination treatment increased T cell expression of checkpoint receptors, with increased PD-1 expression on CD4$^+$ and CD8$^+$ cells and cytotoxic T lymphocyte-associated antigen 4 (CTLA-4) expression on CD8$^+$ cells (Table S1). Again, an increase in tumor-reactive splenocytes was demonstrated by the ELISpot assay (Figure 4C).

Analysis of the injected TME by qRT-PCR demonstrated a significant change toward an inflamed tumor. We observed significant increases in perforin, granzyme B, and IFN-γ (Figures 5A–5C) in the injected tumors, 1 day after the first CpG injection. Meanwhile, we also observed increased mRNA expression levels of tumor necrosis factor alpha (TNF-α), IL-12, and IL-10 (Figures S6A–S6C; Table S2). Immune checkpoint receptors and ligands, including PD-1, PD-L1, and CTLA-4, were increased in the injected tumors (Figures S6D–S6F; Table S2). The untreated TME demonstrated changes 1 day after

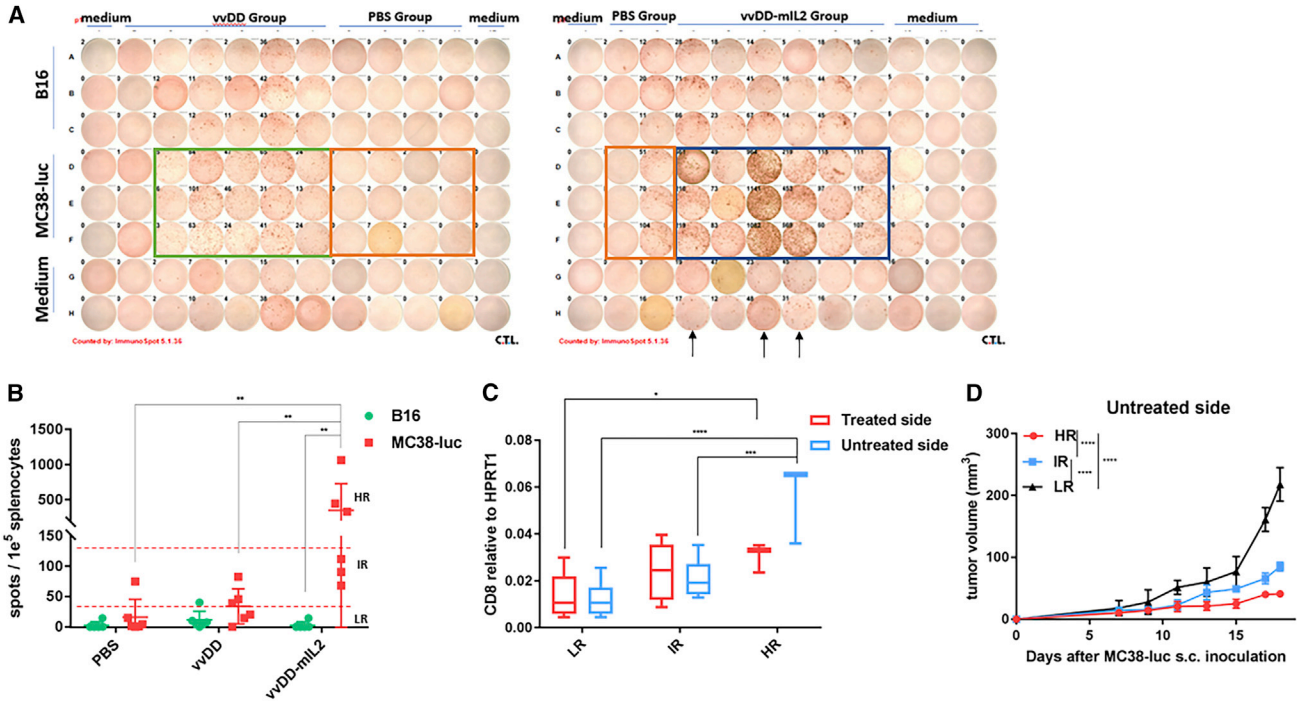

Figure 2. Intratumoral Injection of vvDD-mIL2 Leads to Potent Systemic Immunity That Correlates with CD8 Expression and Anti-tumoral Response in Untreated Tumor

B6 mice were implanted in both flanks with the MC38-luc tumor and sacrificed 8 days after viral delivery into one flank tumor (1.0e8 PFU/50 μL per mouse, n = 6 in each group). (A) ELISpot assay plates are shown using splenocytes stimulated with autologous tumor cells (MC38-luc), control tumor cells (B16), or medium. Arrows show three mice in the vvDD-mIL2 group with exceptionally high levels of IFN-γ secretion after stimulation with autologous tumor cells. (B) Quantities of IFN-γ spots in the different treatment groups, separated into high, intermediate, and low reactivity (HR, IR, and LR, respectively). (C) A qRT-PCR assay was performed to test the expression of CD8 from both sides of HR, IR, and LR mice (regardless of treatment). (D) Virus was injected into one flank tumor on day 11 with 1.0e8 PFU/50 μL per mouse. Tumor growth curve of the untreated side is shown, separated by ELISpot reactivity level to the autologous tumor (HR, IR, and LR mice). Values are mean ± SD. Two-way ANOVA was used to analyze the statistical significance (*$p < 0.05$; **$p < 0.01$; ***$p < 0.001$; ****$p < 0.0001$).

the second CpG injection (2 days later), with increased CD8 mRNA and decreased transforming growth factor beta (TGF-β) and CD105 expression (Figures 5D–5F; Table S2).

We also examined the TME of the injected and untreated tumors using fluorescence-activated cell sorting (FACS), 1 day after the whole therapy was completed. Activated cytotoxic T cells were increased at this point in both the injected and untreated tumors (Figure 5G; Figure S6G) after the dual therapy. Activated helper T cells were also increased in both tumors (Figure 5H). Exhausted cytotoxic T cells were decreased in both tumors (Figure 5I), but Tregs, myeloid-derived suppressor cells, and tumor-associated macrophages (TAMs) were all increased. We also observed more infiltration of natural killer cells (NKs) and DCs in the untreated tumors (Figures 5G–5N). Of note, PD-1$^+$ cytotoxic T cells and T helper cells were highly upregulated in response to dual treatment in both the injected and untreated tumors (Figure S6H). TLR9$^+$ DCs, TAMs, and NKs were also increased in the untreated tumor in response to dual treatment (Figures S6I–S6K). Collectively, these results indicate that the dual therapy of i.t. injection of vvDD-mIL2 and CpG leads to enhanced infiltration of CD4$^+$ and CD8$^+$ T cells, with elevated activation markers, as well as reduced exhausted CD8$^+$ T cells and suppressive markers, which dynamically modifies the TME, thereby enhancing its systemic effect.

In Situ Vaccination Depends on CD8$^+$ T Cells and IFN-γ, whereas Systemic Depletion of Macrophages and PD-1 Blockade Dramatically Enhances the Anti-tumor Response

We performed *in vivo* depletion assays to examine the role of CD4$^+$ and CD8$^+$ T cells and IFN-γ in the anti-tumor effect. The MC38 colon cancer-bearing mice receiving the dual therapy were injected with depletion reagents, as per previous experiments (Figure S7A).[25] The mice receiving either anti-CD8 antibody (Ab) or anti-IFN-γ Ab demonstrated increased tumor growth and died faster than those receiving the dual therapy without depletion. CD4 depletion, however, had no effect (Figures S8A and S8B).

We showed the absolute numbers of immune cell subsets in the untreated tumor with the purpose of demonstrating the relative number of different cell types. PD-1$^+$CD8$^+$ and CD4$^+$ T cells were the most prevalent, followed by TAMs (Figure 6A). All were the highest after combined treatment with vvDD-mIL2 plus CpG. As binding of

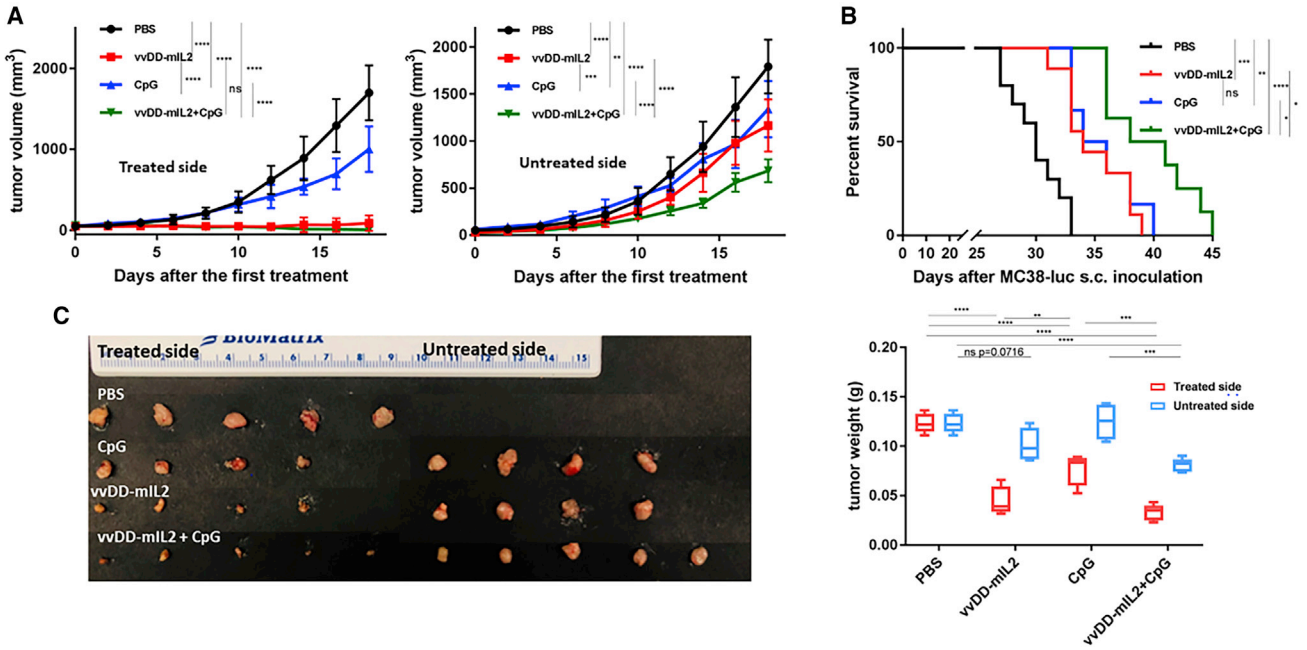

Figure 3. Intratumoral Injection of vvDD-mIL2 Plus the TLR9 Ligand Markedly Improves the Efficacy of *In Situ* Therapeutic Vaccination

B6 mice were inoculated subcutaneously into both flanks with 5.0e5 MC38-luc cancer cells and divided into equal groups according to tumor size. Mice were treated with PBS (50 μL) (n = 10), vvDD-mIL2 (1.0e8 PFU per 50 μL) (n = 9), CpG (50 μg in 50 μL) (n = 6), or virus plus CpG (n = 8) as a local injection into one flank tumor. CpG was injected every other day for a total of three doses on day 3 after virus injection. (A) The graphs represent a comparison of tumor growth in both sides, separated by different treatment groups. (B) The survival of tumor-bearing mice was monitored using Kaplan-Meier analysis, and statistical analyses were performed with log rank test. (C) B6 mice were sacrificed 1 day after the second injection of CpG, and tumor nodules were collected, photographed, and weighed. Values are presented as mean ± SD. Two-way ANOVA was used to analyze the data (*p < 0.05; **p < 0.01; ***p < 0.001; ****p < 0.0001; and ns, not significant).

PD-1 to PD-L1 and TAM activity can both inhibit the immune response, we tested the systemic depletion of macrophages (especially alternatively activated macrophage [M2] phenotype) using clodronate liposomes[40,41] and blocked PD-L1 binding using anti-PD-1 antibody (Figures S7B and S9). We found that clodronate liposome-mediated depletion of macrophages plus anti-PD-1 intraperitoneal injection combined with *in situ* vaccination dramatically reduced the tumor burden on both sides and increased median survival by 87% compared to PBS treatment (three of six mice were tumor free on both sides, 80 days after tumor inoculation), demonstrating that systemic immune adjuvants addressing the suppressive components of the tumor immune microenvironment improve the overall results (Figures 6B and 6C).

DISCUSSION

For a local virus injection to work effectively in patients with metastatic cancer, it must have systemic effects. This can be accomplished through the generation of potent, systemic anti-tumoral immunity using the local viral infection as an *in situ* vaccine.[42] For treatment of a widely metastatic disease, it would be ideal to treat one major tumor mass and then rely on systemic anti-tumoral immunity, thus generated to eliminate distant, untreated nodules. This *in situ* vaccination is a promising approach to immunotherapy.[2,3,43–45] Our current study was aimed toward preclinical modeling and optimization of this systemic anti-tumoral immunity or so-called "abscopal effect" for therapeutic action on untreated distant tumor nodules. We showed in this study that i.t. injection of an IL-2-armed oncolytic VV plus a TLR9 agonist CpG ODN generated potent and sustained systemic anti-tumoral immunity, which led to inhibition of untreated tumor nodules in models of colon and lung cancers in mice.

The OV itself is a multi-mechanistic agent, working first through the lysis of infected cancer cells and associated endothelial cells in the TME.[10,11,44,46] This process of oncolysis releases danger signals and provides tumor antigens (neoantigens included) to the innate immune cells, especially DCs, which cross present tumor antigens to T cells, leading to anti-tumoral immunity. IL-2 was expressed as a membrane-bound active form, which has previously been shown to function as soluble IL-2 but to stay predominately within the TME. The presentation of IL-2 anchored on the cell membranes of the infected cancer cells leads to expansion and activation of T cells within the TME and draining lymph nodes.[9] These T cells circulate systemically and can impact the growth of metastatic tumors.[2,5] This mechanism is supported by our data, where this armed OV induced many changes in the treated tumor favorable for the generation and maintenance of anti-tumoral immunity, including enhanced numbers of activated $CD4^+$ T cells and $CD8^+$ T cells and reduced exhausted $CD8^+$ T cells. We also observed increased tumor-reactive T cells in the splenocytes.

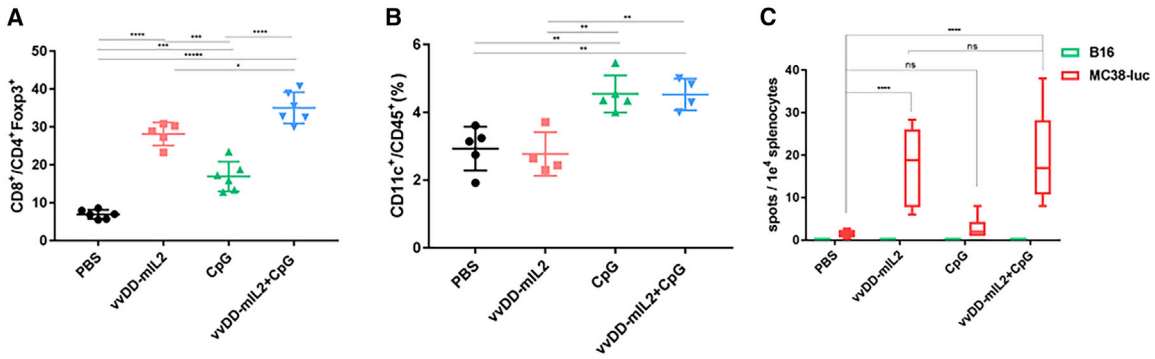

Figure 4. *In Situ* Vaccination Significantly Increases the CD8⁺ T Cell/Treg Ratio and CD11c⁺ Cells in the Spleen

B6 mice were implanted in both flanks with the MC38-luc tumor and sacrificed 1 day after the whole therapy was completed. The spleens were harvested for flow cytometry and an ELISpot assay. (A) Ratio of $CD8^+$ T/Tregs in the spleen. (B) Percentage of $CD11c^+$ in $CD45^+$ splenocytes in four treatment groups. (C) ELISpot assay results using splenocytes stimulated by autologous (MC38-luc) or control (B16) tumor cells. Values represent mean ± SD. One-way ANOVA was used to analyze the statistical significance (*$p < 0.05$; **$p < 0.01$; ***$p < 0.001$; ****$p < 0.0001$).

Although it was beyond the scope of this study to examine every possible immune adjuvant and every possible control, we briefly explored local injections of combinations of CpG ODN, anti-PD-1, and OX40 agonist antibody as additional local adjuvants to improve the viral response in the untreated tumor. The addition of CpG ODN appeared to improve the response, but anti-PD-1 or the OX40 agonist provided no additional benefit when i.t. injected. The TLR9 agonist CpG ODN has been well studied in cancer treatment, and its mechanisms of action in innate immunity, including B cell and DC activation, have been well documented.[30,47] As forementioned, TLR9 signaling may reduce the expression of PD-1 on activated $CD8^+$ T cells, thus reduce exhaustion of activated tumor-specific cytotoxic T lymphocytes (CTLs).[35,36] In the current study, CpG ODN had minimal therapeutic effect in these two tumor models by itself at the recommended dose and scheduling. At the cellular level, it increased the ratio of cytotoxic T cells to Tregs and expanded the number of DCs ($CD11c^+$ cells) in the spleen. In the treated tumor, it enhanced activated T cells (IFN-γ^+CD4^+ and IFN-γ^+CD8^+ T cells) and reduced exhausted T cells (CTLA-4^+PD-1^+CD8^+). Similar patterns of modulation were observed in the untreated nodules, even though the magnitudes were reduced. Generally speaking, when compared to vvDD-mIL2, CpG alone resulted in lower magnitudes of increase in inflammatory factors or reduction in suppressive factors. In the dual-therapy regimen, the positive effects of these two components were usually additive and sometimes synergistic. Together, they achieve the optimal enhancement of anti-tumoral immune cells and reduction of immunosuppressive and exhausted immune cells in the tumor nodules. In the end, the dual therapy reached the best therapeutic outcomes.

This improved effect with combined injections of vvDD-mIL2 and CpG may be related to the effect of CpG on DCs. VV is known to infect DCs and inhibit DC function as a means to its own survival in the host.[48,49] Activation of DCs by CpG may compensate for this inhibition and ultimately improve inflammatory cytokine release in the TME.[34] We did not focus on the effect of NKs in this model, which may contribute anti-tumor activity. Whereas NKs were increased by the combination treatment, their overall numbers were negligible compared to activated T cells. Previous work has demonstrated that inhibition of NKs did not impact the activity of vvDD-mIL2.[9] Finally, we found synergistic increases in $TLR9^+$ DCs, $TLR9^+$ NKs, and $TLR9^+$ TAMs with the combination of OV and CpG without any significant increase with either agent alone. This increase in $TLR9^+$ cells may improve the inflammatory response to repeated CpG treatment and explain why the two agents function well together.

Examination of the tumor immune microenvironment in the untreated tumor was informative and perhaps the most unique aspect of this study. Of note, in our study, the contralateral tumor was implanted at the same time as the injected tumor, so they had the same suppressive immune microenvironment at baseline. This represents a more stringent model compared to others in the literature.[23,26] Despite the virus and CpG staying within the injected tumor, the untreated contralateral tumor changed its cancer-immune set point with about a 2-day delay from changes in the injected tumor. The untreated tumor demonstrated an increase in activated cytotoxic and helper T cells; increased activated DCs and NKs; and decreased exhausted T cells, TGF-β, and CD105, consistent with an immunologically inflamed tumor. The development of systemic anti-tumoral immune reactivity correlates with these findings, suggesting that an active immunization strategy can work to impact untreated metastatic tumors.

We observed upregulation of macrophages in the untreated tumor after injection of virus plus CpG in the contralateral tumor. Macrophages represent the dominant portion of infiltrating leukocytes in all tumors, where they are defined as TAMs and are mostly characterized by an M2-like phenotype.[50] These TAMs facilitate tumor progression by promoting angiogenesis and creating an immunosuppressive environment.[51,52] Clinical trials targeting recruitment, survival, and polarization of TAMs are in progress.[51] The knowledge that these suppressive cells were upregulated led us to test a systemic inhibitor

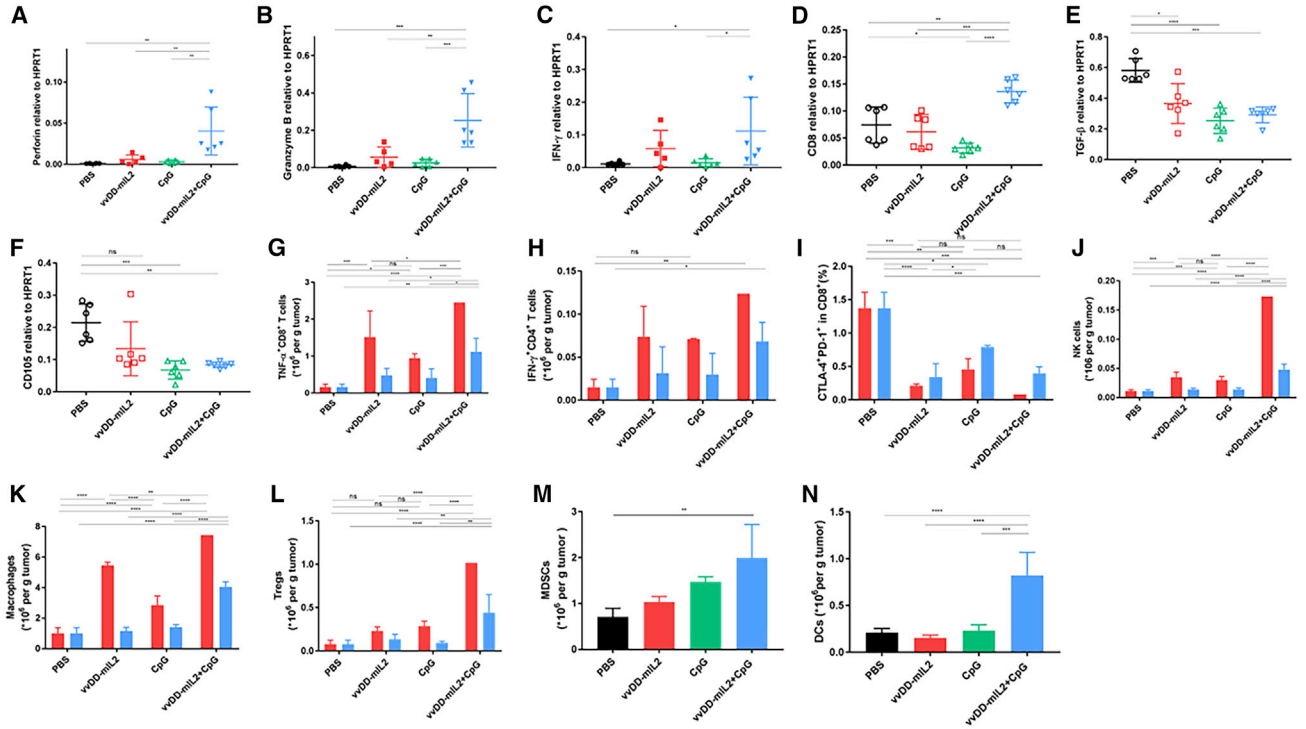

Figure 5. The TME Is Dynamically Modified Post-dual Therapy

(A–F) MC38-luc tumor-bearing mice were sacrificed 1 day after the first or second injection of CpG in different groups (n = 6 in each group), and tumor nodules on both sides were collected and digested for qRT-PCR to explore the cancer-immune set point. The expression levels of all markers are relative to the housekeeping gene, HPRT1. (A–C) Results show the levels of perforin (A), granzyme B (B), and IFN-γ (C), 1 day after the first injection of CpG in the treated side. (D–F) 1 day after the second injection of CpG, the levels of CD8 (D), TGF-β (E), and CD105 (F) from the untreated side are also presented. (G–N) MC38-luc tumor-bearing mice were euthanized 1 day after finishing the whole treatment, and tumor nodules from both sides were collected and lysed for flow cytometry to analyze the TME. Data are quantified (n = 8 in each group). (G–L) Quantities of activated TNF-α^+CD8$^+$ T cells (G) and IFN-γ^+CD4$^+$ T cells (H); the ratio of more severely exhausted PD-1$^+$CTLA-4$^+$CD8$^+$ T cells (I); and quantities of NKs (defined as CD45$^+$CD3$^-$NK1.1$^+$) (J), macrophages (defined as CD45$^+$CD11b$^+$ F4/80$^+$) (K), and Tregs (defined as CD45$^+$CD4$^+$FOXP3$^+$) (L) from both sides are shown. (M and N) On the untreated side, the number of myeloid-derived suppressor cells (MDSCs) (defined as CD45$^+$CD11b$^+$Gr-1$^+$) (M) and DCs (defined as CD45$^+$CD11c$^+$) (N) is also presented. Values are presented as mean ± SD. Two-way ANOVA was used to analyze the data from (G) to (L). One-way ANOVA was used to analyze the statistical significance in other panels (*$p < 0.05$; **$p < 0.01$; ***$p < 0.001$; ****$p < 0.0001$; and ns, not significant).

of macrophage function to improve the response to our local injection. Our results showed that depletion of TAMs (especially the M2 phenotype) enhanced therapeutic efficacy in the untreated tumor. The mechanism of action is multifactorial, but the depletion of TAMs has been shown to inhibit angiogenesis and modulate inflammatory cytokines.[53] Similarly, PD-1 expressing T cells were highly upregulated in the untreated TME in response to vvDD-mIL2 plus CpG injection into the contralateral tumor. The addition of anti-PD-1 therapy further enhanced the response. Rabkin and associates[54] have provided another innovative way to covert M2 TAMs into a classically activated macrophage (M1)-like phenotype in the context of oncolytic immunotherapy, by expressing the cytokine IL-12 from an OV. IL-12 has been shown to possess the capacity to convert M2 TAMs into the M1 phenotype.[55–57] In that study, because it was inhibiting M1 TAMs, clodronate had the opposite effect on the anti-tumor response.

The complex tumor immune microenvironment requires a multifaceted approach to harness the host's immune system successfully and accomplish successful immunotherapy, especially in noninflamed tumors. Our study defines a dual-combination regimen that functions as an *in situ* vaccine to recruit and activate both innate and adaptive immune components, elicit systemic anti-tumor immunity, and stimulate immune-mediated responses in untreated tumor nodules. With the careful examination of the immune microenvironment in untreated tumors, we identified increased TAMs and PD-1/PD-L1 as suppressive factors that inhibited the systemic activity of the vaccine. With the combination of *in situ* vaccination with systemic treatment inhibiting TAMs and PD-1/PD-L1 binding, a successful systemic immunotherapy approach was possible. This approach maximizes the adaptive immunity targeting the tumor without the need to identify specific antigens[44] and therefore, is practical on a large scale. It is agnostic to tumor histology, as the *in situ* procedure utilizes natural antigen processing from tumor cell lysis and requires access to only one tumor mass in the body for a systemic response. It may work as an injection into primary tumors prior to surgical resection, inducing a T cell response to prevent recurrence from micro-metastatic disease. Recent studies with OVs have

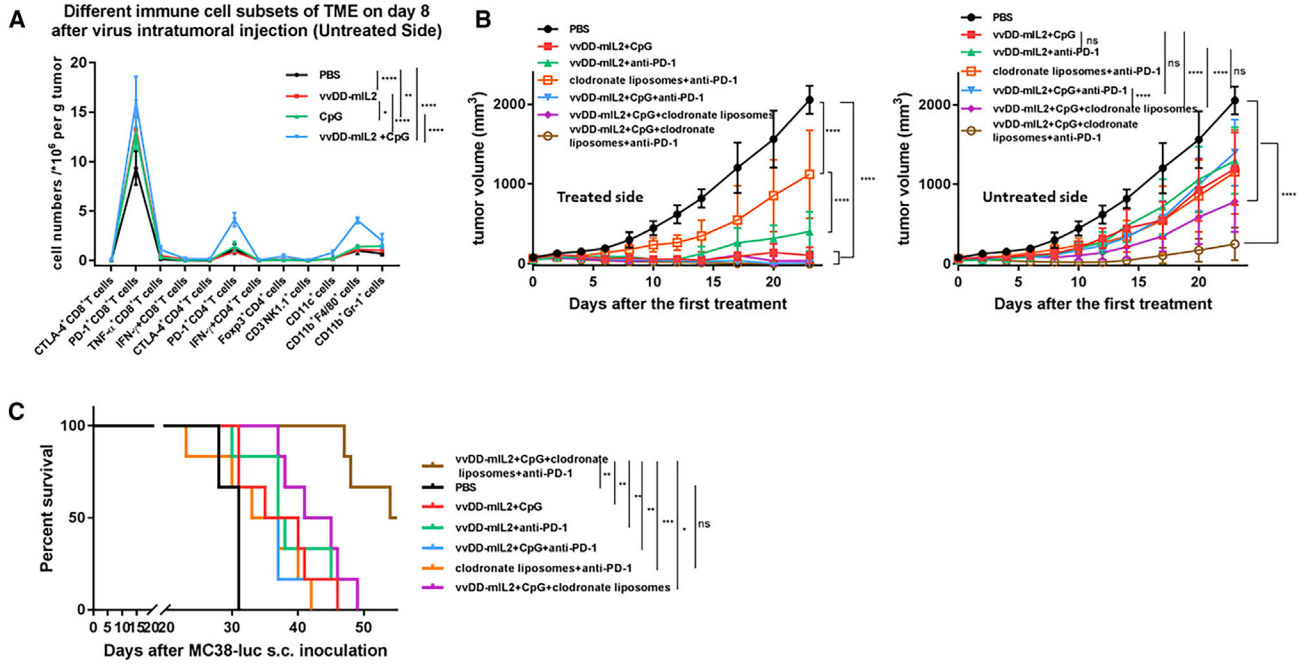

Figure 6. Systemic Depletion of Macrophages and Anti-PD-1 Treatment Dramatically Enhance the Anti-tumoral Response after Local Therapy with vvDD-mIL2 and CpG

(A) Absolute quantities of immune cells in the TME from the untreated side after different treatments (tumors are from the experiment depicted in Figures 5G–5N). (B) B6 mice were inoculated in both flanks with 5.0e5 MC38-luc cancer cells and treated with different regimens, including local injection of vvDD-mIL2 plus CpG and systemic macrophage depletion and anti-PD-1 therapy. The tumor growth curves on both sides are shown. (C) Overall survival was monitored by Kaplan-Meier analysis and analyzed using the log rank test. Three of six mice are still alive 80 days after s.c. tumor cell inoculation. Data are quantified (n = 6 per group). Values are mean ± SD. Two-way ANOVA was used to analyze the statistical significance (*p < 0.05; **p < 0.01; ***p < 0.001; ****p < 0.0001; and ns, not significant). The data represented two independent experiments.

revealed diverse therapeutic response patterns when combining an OV with checkpoint blockade.[23,25,58–61] Therefore, ultimately, these new regimens must move to clinical trials with careful assessment of the tumor immune microenvironment to establish the best approach in patients with poorly immunogenic and multiple-site tumors.

MATERIALS AND METHODS

Cell Lines

Murine colon cancer MC38-luc, melanoma B16, and Lewis lung cancer cells have all been used in our previous studies.[9,62] All mammalian cells listed here were grown in Dulbecco's modified Eagle's medium, supplemented with 10% fetal bovine serum (FBS), 2 mM L-glutamine, and penicillin/streptomycin (Invitrogen, Carlsbad, CA, USA) in a 37°C, 5% CO_2 incubator.

Recombinant Vaccinia Viruses

All recombinant VVs were derived from the Western Reserve (WR) strain. The two viruses vvDD-yellow fluorescent protein (YFP; shortened to vvDD) and vvDD-mIL2-RG (shortened to vvDD-mIL2) have been described previously.[9] vvDD-mIL2 expresses a genetically engineered murine IL-2 that is anchored on the cell surface of the virus-infected cells instead of secretion so that its toxicity is greatly diminished, and thus it is a safer OV.

Mice and Murine Tumor Models

Six-week-old female C57BL/6J strain mice (B6 in short) were purchased from The Jackson Laboratory (Bar Harbor, ME, USA). These mice were housed and fed in specific pathogen-free conditions in the University of Pittsburgh Medical Center (UPMC) Hillman Cancer Center Animal Facility. Animal studies were approved by the University of Pittsburgh Institutional Animal Care and Use Committee.

To establish a s.c. MC38 colon cancer model, B6 mice were inoculated subcutaneously with 5.0e5 MC38-luc cells in 60 μL volume on bilateral flanks and randomly divided into required groups. For pilot experiments, PBS, vvDD, or vvDD-mIL2 was i.t. injected at one nodule with 1.0e8 plaque-forming units (PFU)/50 μL when both s.c. tumor nodules reached ~5 × 5 mm^2. Tumor nodules on both flanks and spleens were collected and analyzed on days 2, 5, 8, and 11 post-initial treatment. For combination therapy studies, 5.0e5 MC38-luc cells in 60 μL were s.c. injected in both flanks of B6 mice. PBS, unmethylated CG-enriched oligodeoxynucleotide (CpG) (ODN 1826; AdipoGen Life Sciences; 50 μg per injection), anti-mouse OX40 (CD134) (clone OX86; Bio X Cell; 8.46 μg per injection) (showed as OX86), anti-PD-1 monoclonal antibody (mAb) (clone RMP1-14; Bio X Cell; 50 μg per injection), vvDD-mIL2 (1.0e8 PFU/50 μL), CpG with vvDD-mIL2, OX86 with vvDD-mIL2, anti-PD-1 with vvDD-mIL2, and

vvDD-mIL2 with CpG and anti-PD-1 mAb were injected i.t. into mice at indicated time points. At some time points, mice were sacrificed to harvest s.c. tumor nodules on both sides, as well as spleens for analyses. In an additional experiment, rat anti-mouse mAbs were intraperitoneally injected into mice to deplete $CD8^+$ T cells or $CD4^+$ T cells or neutralize circulating IFN-γ, according to the following scheme: anti-CD8 Ab (clone 53-6.7; Bio X Cell; 250 μg per injection), anti-CD4 Ab (clone GK1.5; Bio X Cell; 150 μg per injection), anti-IFN-γ Ab (clone XMG1.2; Bio X Cell; 200 μg per injection). Clodronate liposomes (C-010; Liposoma; 200 μL for the first injection but 180 μL for the following three injections) were injected via tail vein to deplete macrophages. For the Lewis lung cancer s.c. tumor model, B6 mice were s.c. injected with 1.0e6 cells in both flanks and i.t. treated with PBS, CpG, vvDD-mIL2, or CpG plus vvDD-mIL2 using the same conditions.

Tumor growth was monitored via digital caliper every other day, and tumor volume was calculated as the following: V (mm^3) = 0.5 × (length × $width^2$). Mice were sacrificed when one of the tumors reached 2,000 mm^3 in size, became ulcerated, and/or interfered with murine activity.

IFN-γ ELISpot Assay

Splenocytes were isolated from MC38-luc tumor-bearing mice, 2, 5, 8, and 11 days post-viral therapy. These splenocytes (1.0e6 cells per mL) were restimulated with 200 Gy irradiated MC38-luc or B16 cells (tumor-specific control) (2.0e5 cells per mL) in 200 μL RPMI-1640 medium, supplemented with 10% FBS at 37°C, 5% CO_2, for 24 h. After incubation, microplates were thoroughly washed before incubating with biotinylated α-mouse IFN-γ Ab overnight (mAb R4-GA2-biotin; Mabtech, Cincinnati, OH, USA). ELISpot plates were then processed, according to vendor protocols for Vectastain Elite ABC (avidin-biotin complex) and AEC (3-amino-9-ethylcarbazole) peroxidase substrate (SK-4200) kits (Vector Laboratories, Burlingame, CA, USA). ImmunoSpot analyzer (Cellular Technology, Shaker Heights, OH, USA) was used to record the data and analyze the results.

Flow Cytometry

Spleens and collected tumor nodules were weighed and incubated in RPMI-1640 medium containing 2% FBS, 1 mg per mL collagenase IV (Sigma; #C5138), 0.1 mg hyaluronidase (Sigma; #H6254), and 200 U DNase I (Sigma; #D5025) at 37°C for 1–2 h to make single cells. Then, these single cells from tumor nodules or spleens were blocked with α-CD16/32 Ab (clone 93; eBioscience; #14-0161-85; 1:1,000) and stained with antibodies against mouse CD45 (PerCP-Cy5.5, clone: 30-F11; BioLegend; #103132; 1:300), CD4 (fluorescein isothiocyanate [FITC], clone: GK1.5; BD Biosciences; #553729; 1:300), Foxp3 (phycoerythrin [PE], clone: FJK-16 s; eBioscience; #12-5773-82; 1:100), CD8 (FITC, clone: 53-6.7; BioLegend; #100706; 1:300), PD-1 (PE, clone: J43; eBioscience; #12-9985-83; 1:300), CTLA-4 (allophycocyanin [APC], clone: UC10-4B9; eBioscience; #17-1522-82; 1:300), IFN-γ (APC, clone: XMG1.2; eBioscience; #17-7311-82; 1:100), TNF-α (PE, clone: MP6-XT22; BioLegend; #506306; 1:300), CD3 (FITC, clone: 17A2; eBioscience; #11-0032-82; 1:300), NK1.1 (APC, clone: PK136; BioLegend; #108710; 1:300), CD11b (FITC, clone: M1/70; BioLegend; #101206; 1:300), CD11c (APC, clone: N418; eBioscience; #17-0114-82; 1:300), Gr-1 (APC, clone: RB6-8C5; eBioscience; #17-5931-82; 1:300), F4/80 (APC, clone: BM8; Fisher Scientific; #50-112-9524; 1:300), CD206 (PE, clone: 19.2; eBioscience; #12-2069-42; 1:20), and TLR9 (PE, clone: J15A7; BD Pharmingen; #565640; 1:300). The intracellular Foxp3, IFN-γ, and TNF-α staining kit was purchased from BioLegend. Samples were collected on a BD Accuri C6 cytometer, and BD Accuri C6 cytometer software was used to analyze data.

qRT-PCR

Total RNA was extracted from tumor nodules using the RNeasy Kit (QIAGEN, Valencia, CA, USA). Normally, 1.0 μg of total RNA was used for cDNA synthesis, and 25 to 50 ng of subsequent cDNA was used for TaqMan gene expression analysis on the StepOnePlus system (Thermo Fisher Scientific, Waltham, MA, USA). We purchased all of the primers for the analysis from Thermo Fisher Scientific. Gene expression was normalized to the housekeeping gene HPRT1 and expressed as fold increase ($2^{-\Delta CT}$), where $\Delta CT = CT_{(\text{target gene})} - CT_{(HPRT1)}$.

Statistics

GraphPad Prism software (GraphPad, San Diego, CA, USA) was used to process raw data, and one-way and two-way ANOVAs were used to analyze the data. Values are presented as mean ± SD. Animal survival is presented using Kaplan-Meier survival curves and was statistically analyzed using the log-rank test. We considered the value $p < 0.05$ to be significant. All p values were assessed two sided. These standard symbols are applied to the figures as the following: *$p < 0.05$; **$p < 0.01$; ***$p < 0.001$; ****$p < 0.0001$; and ns, not significant ($p \geq 0.05$).

SUPPLEMENTAL INFORMATION

Supplemental Information can be found online at https://doi.org/10.1016/j.omto.2020.04.006.

AUTHOR CONTRIBUTIONS

W.L. conducted most of the experiments and collected the data. E.D., Z.L., and C.M. participated in some of the experiments. Z.S.G. and D.L.B. conceived the project. W.L., Z.S.G., and D.L.B. designed the experiments, interpreted the data, and wrote the manuscript.

CONFLICTS OF INTEREST

The authors declare no competing interests.

ACKNOWLEDGMENTS

We thank Ms. Christine Burr for her critical reading and polishing of the manuscript. This research project has been performed at the University of Pittsburgh. W.L. worked at the University of Pittsburgh during September 2017 to August 2019. W.L. and E.D. were supported by fellowships from the China Scholarship Council, China. This work was supported, in part, by the UPMC Immune Transplant and Therapy Center. This project has used the University of Pittsburgh shared core facilities (including the Animal Facility, Genomics

Research Core, and Flow Cytometry), which are supported, in part, by NIH award P30CA047904.

REFERENCES

1. Andtbacka, R.H., Kaufman, H.L., Collichio, F., Amatruda, T., Senzer, N., Chesney, J., Delman, K.A., Spitler, L.E., Puzanov, I., Agarwala, S.S., et al. (2015). Talimogene laherparepvec improves durable response rate in patients with advanced melanoma. J. Clin. Oncol. *33*, 2780–2788.
2. Hammerich, L., Binder, A., and Brody, J.D. (2015). In situ vaccination: Cancer immunotherapy both personalized and off-the-shelf. Mol. Oncol. *9*, 1966–1981.
3. Aznar, M.A., Tinari, N., Rullán, A.J., Sánchez-Paulete, A.R., Rodriguez-Ruiz, M.E., and Melero, I. (2017). Intratumoral Delivery of Immunotherapy-Act Locally, Think Globally. J. Immunol. *198*, 31–39.
4. Locy, H., de Mey, S., de Mey, W., De Ridder, M., Thielemans, K., and Maenhout, S.K. (2018). Immunomodulation of the Tumor Microenvironment: Turn Foe Into Friend. Front. Immunol. *9*, 2909.
5. Bartlett, D.L., Liu, Z., Sathaiah, M., Ravindranathan, R., Guo, Z., He, Y., and Guo, Z.S. (2013). Oncolytic viruses as therapeutic cancer vaccines. Mol. Cancer *12*, 103.
6. Guo, Z.S., Liu, Z., and Bartlett, D.L. (2014). Oncolytic immunotherapy: dying the right way is a key to eliciting potent antitumor immunity. Front. Oncol. *4*, 74.
7. Workenhe, S.T., and Mossman, K.L. (2014). Oncolytic virotherapy and immunogenic cancer cell death: sharpening the sword for improved cancer treatment strategies. Mol. Ther. *22*, 251–256.
8. Chen, D.S., and Mellman, I. (2017). Elements of cancer immunity and the cancer-immune set point. Nature *541*, 321–330.
9. Liu, Z., Ge, Y., Wang, H., Ma, C., Feist, M., Ju, S., Guo, Z.S., and Bartlett, D.L. (2018). Modifying the cancer-immune set point using vaccinia virus expressing re-designed interleukin-2. Nat. Commun. *9*, 4682.
10. Gujar, S., Bell, J., and Diallo, J.-S. (2019). SnapShot: Cancer Immunotherapy with Oncolytic Viruses. Cell *176*, 1240–1240.e1.
11. Guo, Z.S., Lu, B., Guo, Z., Giehl, E., Feist, M., Dai, E., Liu, W., Storkus, W.J., He, Y., Liu, Z., and Bartlett, D.L. (2019). Vaccinia virus-mediated cancer immunotherapy: cancer vaccines and oncolytics. J. Immunother. Cancer *7*, 6.
12. Torres-Domínguez, L.E., and McFadden, G. (2019). Poxvirus oncolytic virotherapy. Expert Opin. Biol. Ther. *19*, 561–573.
13. McCart, J.A., Ward, J.M., Lee, J., Hu, Y., Alexander, H.R., Libutti, S.K., Moss, B., and Bartlett, D.L. (2001). Systemic cancer therapy with a tumor-selective vaccinia virus mutant lacking thymidine kinase and vaccinia growth factor genes. Cancer Res. *61*, 8751–8757.
14. Parato, K.A., Breitbach, C.J., Le Boeuf, F., Wang, J., Storbeck, C., Ilkow, C., Diallo, J.S., Falls, T., Burns, J., Garcia, V., et al. (2012). The oncolytic poxvirus JX-594 selectively replicates in and destroys cancer cells driven by genetic pathways commonly activated in cancers. Mol. Ther. *20*, 749–758.
15. Zeh, H.J., Downs-Canner, S., McCart, J.A., Guo, Z.S., Rao, U.N., Ramalingam, L., Thorne, S.H., Jones, H.L., Kalinski, P., Wieckowski, E., et al. (2015). First-in-man study of western reserve strain oncolytic vaccinia virus: safety, systemic spread, and antitumor activity. Mol. Ther. *23*, 202–214.
16. Downs-Canner, S., Guo, Z.S., Ravindranathan, R., Breitbach, C.J., O'Malley, M.E., Jones, H.L., Moon, A., McCart, J.A., Shuai, Y., Zeh, H.J., and Bartlett, D.L. (2016). Phase 1 study of intravenous oncolytic poxvirus (vvDD) in patients with advanced solid cancers. Mol. Ther. *24*, 1492–1501.
17. Bommareddy, P.K., Shettigar, M., and Kaufman, H.L. (2018). Integrating oncolytic viruses in combination cancer immunotherapy. Nat. Rev. Immunol. *18*, 498–513.
18. Twumasi-Boateng, K., Pettigrew, J.L., Kwok, Y.Y.E., Bell, J.C., and Nelson, B.H. (2018). Oncolytic viruses as engineering platforms for combination immunotherapy. Nat. Rev. Cancer *18*, 419–432.
19. Pearl, T.M., Markert, J.M., Cassady, K.A., and Ghonime, M.G. (2019). Oncolytic Virus-Based Cytokine Expression to Improve Immune Activity in Brain and Solid Tumors. Mol. Ther. Oncolytics *13*, 14–21.
20. Toda, M., Rabkin, S.D., Kojima, H., and Martuza, R.L. (1999). Herpes simplex virus as an in situ cancer vaccine for the induction of specific anti-tumor immunity. Hum. Gene Ther. *10*, 385–393.
21. Stojdl, D.F., Lichty, B.D., tenOever, B.R., Paterson, J.M., Power, A.T., Knowles, S., Marius, R., Reynard, J., Poliquin, L., Atkins, H., et al. (2003). VSV strains with defects in their ability to shutdown innate immunity are potent systemic anti-cancer agents. Cancer Cell *4*, 263–275.
22. Kaufman, H.L., Kim, D.W., DeRaffele, G., Mitcham, J., Coffin, R.S., and Kim-Schulze, S. (2010). Local and distant immunity induced by intralesional vaccination with an oncolytic herpes virus encoding GM-CSF in patients with stage IIIc and IV melanoma. Ann. Surg. Oncol. *17*, 718–730.
23. Zamarin, D., Holmgaard, R.B., Subudhi, S.K., Park, J.S., Mansour, M., Palese, P., Merghoub, T., Wolchok, J.D., and Allison, J.P. (2014). Localized oncolytic virotherapy overcomes systemic tumor resistance to immune checkpoint blockade immunotherapy. Sci. Transl. Med. *6*, 226ra32.
24. Fend, L., Yamazaki, T., Remy, C., Fahrner, C., Gantzer, M., Nourtier, V., Préville, X., Quéméneur, E., Kepp, O., Adam, J., et al. (2017). Immune Checkpoint Blockade, Immunogenic Chemotherapy or IFN-α Blockade Boost the Local and Abscopal Effects of Oncolytic Virotherapy. Cancer Res. *77*, 4146–4157.
25. Liu, Z., Ravindranathan, R., Kalinski, P., Guo, Z.S., and Bartlett, D.L. (2017). Rational combination of oncolytic vaccinia virus and PD-L1 blockade works synergistically to enhance therapeutic efficacy. Nat. Commun. *8*, 14754.
26. Bourgeois-Daigneault, M.-C., Roy, D.G., Aitken, A.S., El Sayes, N., Martin, N.T., Varette, O., Falls, T., St-Germain, L.E., Pelin, A., Lichty, B.D., et al. (2018). Neoadjuvant oncolytic virotherapy before surgery sensitizes triple-negative breast cancer to immune checkpoint therapy. Sci. Transl. Med. *10*, eaao1641.
27. Kellish, P., Shabashvili, D., Rahman, M.M., Nawab, A., Guijarro, M.V., Zhang, M., Cao, C., Moussatche, N., Boyle, T., Antonia, S., et al. (2019). Oncolytic virotherapy for small-cell lung cancer induces immune infiltration and prolongs survival. J. Clin. Invest. *129*, 2279–2292.
28. Rajani, K., Parrish, C., Kottke, T., Thompson, J., Zaidi, S., Ilett, L., Shim, K.G., Diaz, R.M., Pandha, H., Harrington, K., et al. (2016). Combination therapy with reovirus and anti-PD-1 blockade controls tumor growth through innate and adaptive immune responses. Mol. Ther. *24*, 166–174.
29. Sagiv-Barfi, I., Czerwinski, D.K., Levy, S., Alam, I.S., Mayer, A.T., Gambhir, S.S., and Levy, R. (2018). Eradication of spontaneous malignancy by local immunotherapy. Sci. Transl. Med. *10*, eaan4488.
30. Krieg, A.M. (2006). Therapeutic potential of Toll-like receptor 9 activation. Nat. Rev. Drug Discov. *5*, 471–484.
31. Kaczanowska, S., Joseph, A.M., and Davila, E. (2013). TLR agonists: our best frenemy in cancer immunotherapy. J. Leukoc. Biol. *93*, 847–863.
32. Lou, Y., Liu, C., Lizée, G., Peng, W., Xu, C., Ye, Y., Rabinovich, B.A., Hailemichael, Y., Gelbard, A., Zhou, D., et al. (2011). Antitumor activity mediated by CpG: the route of administration is critical. J. Immunother. *34*, 279–288.
33. Brody, J.D., Ai, W.Z., Czerwinski, D.K., Torchia, J.A., Levy, M., Advani, R.H., Kim, Y.H., Hoppe, R.T., Knox, S.J., Shin, L.K., et al. (2010). In situ vaccination with a TLR9 agonist induces systemic lymphoma regression: a phase I/II study. J. Clin. Oncol. *28*, 4324–4332.
34. Xiao, H., Peng, Y., Hong, Y., Huang, L., Guo, Z.S., Bartlett, D.L., Fu, N., Munn, D.H., Mellor, A., and He, Y. (2013). Local administration of TLR ligands rescues the function of tumor-infiltrating CD8 T cells and enhances the antitumor effect of lentivector immunization. J. Immunol. *190*, 5866–5873.
35. Wong, R.M., Smith, K.A., Tam, V.L., Pagarigan, R.R., Meisenburg, B.L., Quach, A.M., Carrillo, M.A., Qiu, Z., and Bot, A.I. (2009). TLR-9 signaling and TCR stimulation co-regulate CD8(+) T cell-associated PD-1 expression. Immunol. Lett. *127*, 60–67.
36. Duraiswamy, J., Freeman, G.J., and Coukos, G. (2013). Therapeutic PD-1 pathway blockade augments with other modalities of immunotherapy T-cell function to prevent immune decline in ovarian cancer. Cancer Res. *73*, 6900–6912.
37. Krieg, A.M. (2007). Development of TLR9 agonists for cancer therapy. J. Clin. Invest. *117*, 1184–1194.
38. Aspeslagh, S., Postel-Vinay, S., Rusakiewicz, S., Soria, J.C., Zitvogel, L., and Marabelle, A. (2016). Rationale for anti-OX40 cancer immunotherapy. Eur. J. Cancer *52*, 50–66.

39. Chen, L., and Han, X. (2015). Anti-PD-1/PD-L1 therapy of human cancer: past, present, and future. J. Clin. Invest. *125*, 3384–3391.

40. Zeisberger, S.M., Odermatt, B., Marty, C., Zehnder-Fjällman, A.H., Ballmer-Hofer, K., and Schwendener, R.A. (2006). Clodronate-liposome-mediated depletion of tumour-associated macrophages: a new and highly effective antiangiogenic therapy approach. Br. J. Cancer *95*, 272–281.

41. Griesmann, H., Drexel, C., Milosevic, N., Sipos, B., Rosendahl, J., Gress, T.M., and Michl, P. (2017). Pharmacological macrophage inhibition decreases metastasis formation in a genetic model of pancreatic cancer. Gut *66*, 1278–1285.

42. Spitzer, M.H., Carmi, Y., Reticker-Flynn, N.E., Kwek, S.S., Madhireddy, D., Martins, M.M., Gherardini, P.F., Prestwood, T.R., Chabon, J., Bendall, S.C., et al. (2017). Systemic immunity is required for effective cancer immunotherapy. Cell *168*, 487–502.e15.

43. Morris, Z.S., Guy, E.I., Werner, L.R., Carlson, P.M., Heinze, C.M., Kler, J.S., Busche, S.M., Jaquish, A.A., Sriramaneni, R.N., Carmichael, L.L., et al. (2018). Tumor-Specific Inhibition of *In Situ* Vaccination by Distant Untreated Tumor Sites. Cancer Immunol. Res. *6*, 825–834.

44. Russell, S.J., and Barber, G.N. (2018). Oncolytic Viruses as Antigen-Agnostic Cancer Vaccines. Cancer Cell *33*, 599–605.

45. Hammerich, L., Marron, T.U., Upadhyay, R., Svensson-Arvelund, J., Dhainaut, M., Hussein, S., Zhan, Y., Ostrowski, D., Yellin, M., Marsh, H., et al. (2019). Systemic clinical tumor regressions and potentiation of PD1 blockade with in situ vaccination. Nat. Med. *25*, 814–824.

46. Chaurasiya, S., Chen, N.G., and Fong, Y. (2018). Oncolytic viruses and immunity. Curr. Opin. Immunol. *51*, 83–90.

47. Wu, J., Su, W., Powner, M.B., Liu, J., Copland, D.A., Fruttiger, M., Madeddu, P., Dick, A.D., and Liu, L. (2016). Pleiotropic action of CpG-ODN on endothelium and macrophages attenuates angiogenesis through distinct pathways. Sci. Rep. *6*, 31873.

48. Cunningham, A.L., Donaghy, H., Harman, A.N., Kim, M., and Turville, S.G. (2010). Manipulation of dendritic cell function by viruses. Curr. Opin. Microbiol. *13*, 524–529.

49. Tang, B., Guo, Z.S., Bartlett, D.L., Liu, J., McFadden, G., Shisler, J.L., and Roy, E.J. (2019). A cautionary note on the selectivity of oncolytic poxviruses. Oncolytic Virother. *8*, 3–8.

50. Lewis, C.E., and Pollard, J.W. (2006). Distinct role of macrophages in different tumor microenvironments. Cancer Res. *66*, 605–612.

51. Mantovani, A., Marchesi, F., Malesci, A., Laghi, L., and Allavena, P. (2017). Tumour-associated macrophages as treatment targets in oncology. Nat. Rev. Clin. Oncol. *14*, 399–416.

52. De Palma, M., and Lewis, C.E. (2013). Macrophage regulation of tumor responses to anticancer therapies. Cancer Cell *23*, 277–286.

53. Piaggio, F., Kondylis, V., Pastorino, F., Di Paolo, D., Perri, P., Cossu, I., Schorn, F., Marinaccio, C., Murgia, D., Daga, A., et al. (2016). A novel liposomal Clodronate depletes tumor-associated macrophages in primary and metastatic melanoma: Anti-angiogenic and anti-tumor effects. J. Control. Release *223*, 165–177.

54. Saha, D., Martuza, R.L., and Rabkin, S.D. (2017). Macrophage Polarization Contributes to Glioblastoma Eradication by Combination Immunovirotherapy and Immune Checkpoint Blockade. Cancer Cell *32*, 253–267.e5.

55. Watkins, S.K., Egilmez, N.K., Suttles, J., and Stout, R.D. (2007). IL-12 rapidly alters the functional profile of tumor-associated and tumor-infiltrating macrophages in vitro and in vivo. J. Immunol. *178*, 1357–1362.

56. He, W., Zhu, Y., Mu, R., Xu, J., Zhang, X., Wang, C., Li, Q., Huang, Z., Zhang, J., Pan, Y., et al. (2017). A Jak2-selective inhibitor potently reverses the immune suppression by modulating the tumor microenvironment for cancer immunotherapy. Biochem. Pharmacol. *145*, 132–146.

57. Ma, X., Yan, W., Zheng, H., Du, Q., Zhang, L., Ban, Y., Li, N., and Wei, F. (2015). Regulation of IL-10 and IL-12 production and function in macrophages and dendritic cells. F1000Res. *4*, F1000 Faculty Rev–1465.

58. Engeland, C.E., Grossardt, C., Veinalde, R., Bossow, S., Lutz, D., Kaufmann, J.K., Shevchenko, I., Umansky, V., Nettelbeck, D.M., Weichert, W., et al. (2014). CTLA-4 and PD-L1 checkpoint blockade enhances oncolytic measles virus therapy. Mol. Ther. *22*, 1949–1959.

59. Yan, X., Wang, L., Zhang, R., Pu, X., Wu, S., Yu, L., Meraz, I.M., Zhang, X., Wang, J.F., Gibbons, D.L., et al. (2017). Overcoming resistance to anti-PD immunotherapy in a syngeneic mouse lung cancer model using locoregional virotherapy. OncoImmunology *7*, e1376156.

60. McGray, A.J.R., Huang, R.Y., Battaglia, S., Eppolito, C., Miliotto, A., Stephenson, K.B., Lugade, A.A., Webster, G., Lichty, B.D., Seshadri, M., et al. (2019). Oncolytic Maraba virus armed with tumor antigen boosts vaccine priming and reveals diverse therapeutic response patterns when combined with checkpoint blockade in ovarian cancer. J. Immunother. Cancer *7*, 189.

61. Chon, H.J., Lee, W.S., Yang, H., Kong, S.J., Lee, N.K., Moon, E.S., Choi, J., Han, E.C., Kim, J.H., Ahn, J.B., et al. (2019). Tumor Microenvironment Remodeling by Intratumoral Oncolytic Vaccinia Virus Enhances the Efficacy of Immune-Checkpoint Blockade. Clin. Cancer Res. *25*, 1612–1623.

62. Guo, Z.S., Parimi, V., O'Malley, M.E., Thirunavukarasu, P., Sathaiah, M., Austin, F., and Bartlett, D.L. (2010). The combination of immunosuppression and carrier cells significantly enhances the efficacy of oncolytic poxvirus in the pre-immunized host. Gene Ther. *17*, 1465–1475.